Eur Radiol (2016) 26:664–673
DOI 10.1007/s00330-015-3854-5

MAGNETIC RESONANCE

MR appearance of parathyroid adenomas at 3 T in patients with primary hyperparathyroidism: what radiologists need to know for pre-operative localization

B. Sacconi[1] · R. Argirò[1] · Daniele Diacinti[1,4] · A Iannarelli[1] · M. Bezzi[1] · C. Cipriani[2] · D. Pisani[3] · V. Cipolla[1] · C. De Felice[1] · S. Minisola[2] · C. Catalano[1]

Received: 19 March 2015 / Revised: 30 April 2015 / Accepted: 13 May 2015 / Published online: 31 May 2015

Abstract
Objectives To identify frequent MRI features of parathyroid adenomas (PTAs) in patients with primary hyperparathyroidism (PHPT) using a fast protocol with a 3 T magnet.
Methods Thirty-eight patients with PHPT underwent a 3 T-MR. All patients had positive US and Tc-99 sestamibi, for a total number of 46 PTAs. T2-weighted IDEAL-FSE and T1 IDEA L-sequences, before and after contrast, were performed. Five features of PTAs were recognised: hyperintensity, homogeneous or "marbled" appearance and elongated morphology on T2-sequences; cleavage plane from thyroid gland on T2-outphase; rapid enhancement in post-contrast T1. Image quality for T2-weighted IDEAL FSE and usefulness for IDEAL post-contrast T1-weighted and T2-outphase sequences were also graded.
Results PTAs were hyperintense in T2-sequences in 44/46 (95.7 %), "marbled" in 30/46 (65.2 %) and elongated in 38/46 (82.6 %) patients. Cleavage plane was observed in 36/46 (78.3 %), and rapid enhancement in 20/46 (43.5 %) patients. T2-sequences showed both excellent fat suppression and image quality (average scores of 3.2 and 3.1). T2-outphase images demonstrated to be quite useful (score 2.8), whereas, post-contrast T1 images showed a lower degree of utility (score 2.4).
Conclusions A fast protocol with 3.0-T MRI, recognising most common features of PTAs, may be used as a second-line method in the preoperative detection of PTAs.
Key Points
- *3 T MRI protocol based on T2-weighted IDEAL FSE sequences was used.*
- *T2-hyperintensity and elongated morphology are common features of PTAs.*
- *3 T MRI could be used in the preoperative detection of PTAs.*

Keywords Parathyroid adenoma · 3 T Magnetic Resonance Imaging · IDEAL sequences · Presurgical localisation · Primary hyperparathyroidism

Introduction

Primary hyperparathyroidism (PHPT) is characterised by an excess of parathyroid hormone (PTH) secretion, causing hypercalcemia, and occurs in about 1 % of adults [1–3]. PHPT is caused by a single parathyroid adenoma (PTA) in approximately 90 % of patients, and by multiple gland hyperplasia (5 %), double adenomas (4 %), and parathyroid carcinomas (1 %) [4].

Definitive treatment of PHPT is surgical in most cases. National Institutes of Health (NIH) guidelines recommended parathyroidectomy in all symptomatic and asymptomatic patients<50 years of age [5]. More recently, several authors proposed more expansive criteria for surgical therapy, excluding only those patients who are not able to tolerate surgery [6, 7].

✉ Daniele Diacinti
daniele.diacinti@uniroma1.it

[1] Department of Radiological Sciences, Oncology and Pathology, Sapienza University, viale Regina Elena 324, 00161 Rome, Italy

[2] Department of Clinical Sciences, Sapienza University, viale del Policlinico 155, 00161 Rome, Italy

[3] Department of Clinical and Molecular Medicine, Sapienza University, via Grottarossa 1035, 00189 Rome, Italy

[4] Department of Radiological Sciences, Oncology and Pathology, Sapienza Università di Roma, V.le Regina Elena 324, 00161 Roma, Italy

Nevertheless, with the variable number and anatomic location of parathyroid glands, preoperative imaging has rarely been used for traditional open-neck surgery [8–11]. Since 90 % of patients with PHPT have a single gland adenoma, minimally invasive parathyroidectomy (MIP) was introduced [12–14], with decreased intraoperative time, size of surgical incision and complication rates [15, 16]. Accurate preoperative localisation of parathyroid disease is absolutely critical for effective surgical treatment when MIP is used [17, 18], and almost all authors also recommend intraoperative PTH hormone level monitoring [19–21].

Ultrasound (US) and 99mTc-sestamibi scintigraphy are the dominant imaging techniques for preoperative location of PTAs [22–30]. A preoperative approach that combines the anatomic information of US and the functional information of scintigraphy may localise a solitary PTA more accurately (sensitivity of 95 %) than a single technique [31–36].

When first-line modalities fail to localise PTA, computed tomography (CT) is generally proposed as a second line imaging technique to localise PTAs, particularly in the case of ectopic glands in the upper mediastinum or in the case of post-surgical recurrent PHPT [37–39]. Since 2006, a new CT technique, 4D-CT, has been introduced, combining detailed anatomic definition and functional information based on enhancement patterns [40, 41].

As in the case of CT, magnetic resonance imaging (MRI) has been used as second line pre-operative localizing technique, or in the case of persistent post-operative PHPT. MRI has been used with sensitivity at nearly 80 % in most studies using 1.5 T magnets to preoperatively localise PTAs [42–45], or at even higher sensitivities in other studies [46]. The use of 3 T magnets in head and neck MRI introduced some changes of the intrinsic tissue relaxation parameters, improving the preoperative detection of PTA [47]. In particular, at 3 T, the signal-to-noise and the contrast-to-noise ratios are higher, leading to an increased detection of small and hypervascular tissues [48]; an excellent fat saturation can be obtained using 3 T magnets, thanks to chemical shift-based Dixon water–fat separation methods, commercially known as IDEAL (Iterative Decomposition of water and fat with Echo Asymmetry and Least squares estimation) [49–52]. The use of time-resolved imaging of contrast kinetics (TRICKS) [53], on the contrary, resulted in only a modest improvement in PTA detection rates [54]. In most previous studies, only non-specific MR signal features of PTA have been ruled out (such as low T1 signal, strong and fast enhancement and high T2 signal), which do not allow for differential diagnosis of other entities that are often located in the same anatomical sites (lymph nodes and exophytic thyroid nodules) [55–57].

The purpose of our study was to identify recurrent MR features of PTAs in patients with primary HPT, by using a fast imaging protocol with a 3.0-T MRI scanner for preoperative localisation.

Materials and methods

Patients

After obtaining institutional ethic review board approval and informed consent, 38 patients (34 F; average age 65 years, range 22–88) with clinical diagnosis of PHPT were prospectively enrolled in the study between July 2013 and July 2014.

All patients had both positive and concordant US and sestamibi scans performed before the MR examination. US and sestamibi scans localised a total of 46 adenomas, all located in eutopic sites. Previous US and sestamibi evaluations were performed at our Institution or were available for review; thus, all the identified lesions were discussed in our centre by radiologists and nuclear medicine specialists, and were included in the study only in the case of high diagnostic confidence. None of the patients had undergone surgery in the neck region.

Study protocol

Before surgery, all patients underwent an MR examination by a 3 Tesla unit (Discovery MR 750, GE Healthcare, Waukesha, WI, USA) with a dedicated eight-channel neurovascular phased array coil. Field of view was adjusted to include the area from the carotid bifurcation to the level of tracheal carina.

All patients were imaged using a dedicated MRI protocol composed of a three-plane localiser and T2-weighted IDEAL FSE sequences (coronal, sagittal and axial planes).

A T1-weighted IDEAL sequence with the following parameters was then obtained (LAVA FLEX): TR 5 msec, TE 2 msec, FoV 240x300, Matrix 320x224, slice thickness 3.0 mm, acquisition time 18 sec. The same sequence was performed after contrast media administration (0.1 mL/kg of gadobenate dimeglumine, Multihance BRACCO, Milan, Italy, at 2 ml per second followed by a 20-ml saline flush at the same rate); six phases were acquired with an effective temporal resolution of 18 s each, for an overall scan time of 1:48 min. The first post-contrast sequence began monitoring the enhancement in the aortic arch through a fluoro-MR technique. Imaging parameters are summarised in Table 1.

Image review

Two radiologists with 8 and 7 years of experience in head and neck imaging and a fifth year radiology resident reviewed the MRI examinations by simultaneous consensus. The three readers were aware of all other imaging results. Once PTAs were identified by matching US and Tc-99 sestamibi scan locations, the three radiologists evaluated the presence of five features: hyperintensity on T2-weighted IDEAL FSE sequences, homogeneous signal or “marbled” appearance and elongated morphology on T2-weighted IDEAL FSE

Table 1 Scan parameters for 3 T MRI protocol

	TR (msec)	TE (msec)	FoV	Matrix	Slice thickness (mm)	Acquisition time (sec)
T2 IDEAL cor	2060	110	300×300	320×224	3.0	190
T2 IDEAL sag	2497	90	300×300	320×224	3.0	200
T2 IDEAL ax	5066	106	216×240	320×224	3.0	380
T1 IDEAL ax	5	2	240×300	320×224	3.0	18 (×6)

sequences, presence of a cleavage plane between the PTA and the thyroid gland, and rapid enhancement on T1-weighted IDEAL post contrast sequences (Fig. 1).

The evaluation of these features was performed as follows:

- Hyperintensity: subjectively evaluated in comparison with the signal intensity of the normal thyroid gland. In case of doubt, radiologists drew multiple regions of interest (ROIs) in the PTA and in the normal thyroid tissue.
- "Marbled" appearance: a four-point score was used: 1 homogeneous; 2 quite homogeneous; 3 poorly homogeneous; 4 patchy. Glands with a score of 3 and 4 were considered to have a "marbled" appearance.
- Elongated morphology: if the ratio between the longest and the shortest diameter of the gland was≥2.0, then its morphology was considered to be elongated.
- Cleavage plane with the thyroid gland: interposition of an evident fat tissue plane on any sequence or presence of an "India ink" artefact on T2-weighted outphase IDEAL sequences between the PTA and the thyroid gland [58].
- Rapid and strong enhancement in comparison with normal thyroid observed in the first post-contrast sequence:

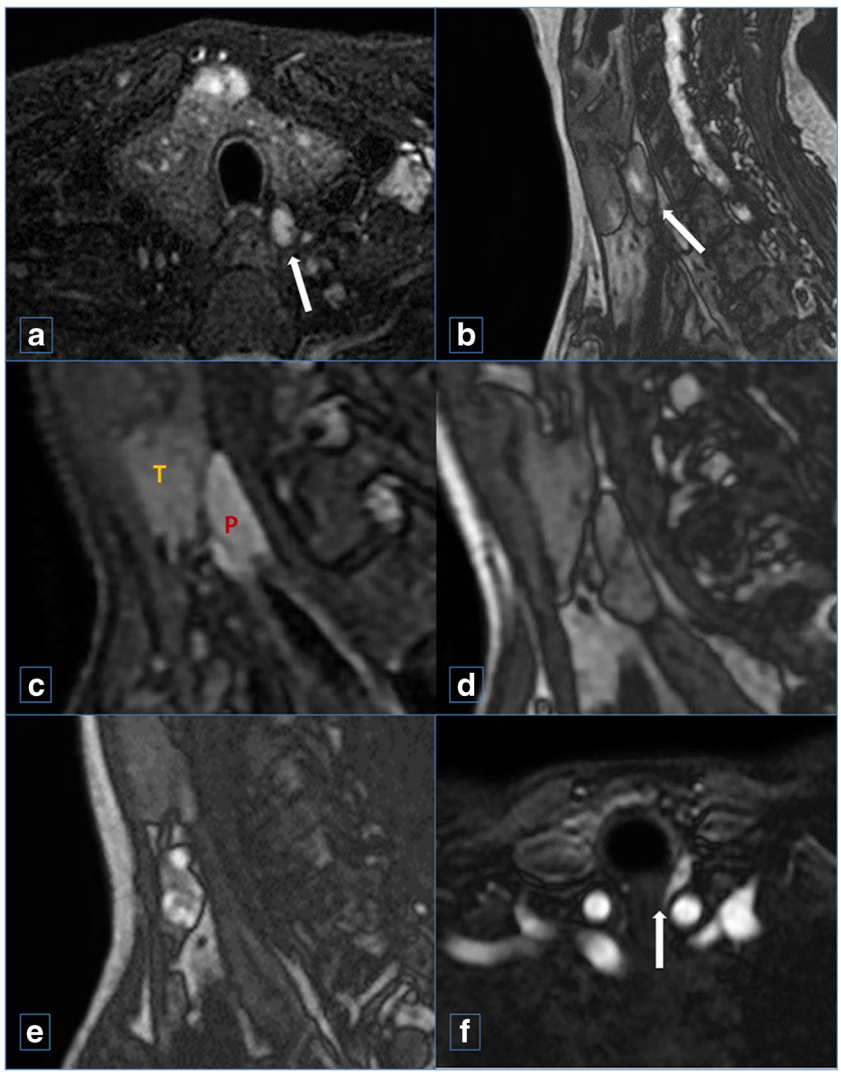

Fig. 1 Intrinsic features of parathyroid adenomas on MR images as described in the text. (*A*) Hyperintensity; (*B*) oblong morphology; (*C*) cleavage plane between the PTA and the thyroid gland, best seen using the *India-Ink artefact*; (*D*) "marbled" aspect; (*E*) fast and strong enhancement on early post-contrast T1WI

in case of doubt, radiologists drew multiple ROIs in the PTA and in the normal thyroid tissue.

Data analysis

The interpretation of the MR was correlated with US and sestamibi results. In addition, image quality for T2-weighted IDEAL FSE sequences and post-contrast T1-weighted IDEAL (LAVA FLEX) sequences was assessed, considering the depiction of PTAs and the presence of artefacts.

T2-weighted IDEAL FSE images were graded on two four-point scales (1=poor, 2=fair, 3=good, 4=excellent) for the quality of fat saturation and overall image quality.

Post-contrast T1-weighted IDEAL images (LAVA FLEX) were graded on a scale from 1 to 4, based on the sequence's capability to identify a vascularised tissue representing a potential PTA. The assessment was performed as follows: 1=not helpful (no enhancement); 2=marginally helpful (enhancement comparable with that of thyroid); 3=very helpful (higher enhancement than thyroid, but PTA was already well depicted by T2-weighted sequences); 4=extremely helpful (higher enhancement than thyroid and PTA was not depicted by T2 weighted sequences). Also T2 IDEAL FSE out-phase sequences were evaluated using the same scale from 1 to 4, with reference to their capability to depict the cleavage plane between PTAs and thyroid gland, using the India Ink artefact or not: 1=not helpful (no cleavage plane); 2=marginally helpful (cleavage plane observed in all the other sequences); 3=very helpful (cleavage plane observed in other sequences, but more accurately depicted in the T2 weighted out-phase sequence); 4=extremely helpful (depiction of a cleavage plane otherwise not identified). The location (left or right, and if possible, superior or inferior gland, as well as any ectopic parathyroid adenoma) was recorded.

For accuracy of interpretation, the PTA had to be identified exactly in the same site suggested by US and sestamibi scans.

Surgical treatment and clinical follow-up

Patients for whom surgery was considered as indicated underwent surgical intervention at our Institution, consisting of minimally invasive surgery or open bilateral neck exploration. Patients for whom surgery was not indicated on the basis of their medical conditions (or patients who refused surgery) received medical therapy and/or clinical/radiological follow-up.

Results

None of the patients enrolled were excluded from the study and all of them underwent a complete MR examination. Total average examination time amounted to around 15 minutes. There were no reported side effects due to the administration of contrast material.

All PTAs (46/46) were identified in the same location described at US and Tc-99 sestamibi scans by three readers in consensus, unblinded to these previous examinations. Twenty-six adenomas were right-sided and 20 were left-sided. MRI confirmed that five patients had multiple enlarged parathyroid glands, localised on both sides. Average lesion size was 14.5x8.5x9.5 mm (range 5–33 mm), and average volume was 771 mm^3 (range 33–5525 mm^3).

High signal intensity on T2-weighted IDEAL FSE images was observed in 44/46 cases (95.7 %), in comparison with that of the thyroid gland (Fig. 2). A marbled aspect (score 3/4) was observed in 30/46 cases (65.2 %); 18 out of these 30 PTAs were larger than 15 mm of maximum diameter (Fig. 3). Elongated morphology was observed in 38/46 cases (82.6 %); the longest diameter usually corresponded to the longitudinal diameter of the enlarged gland, whereas the shortest diameter corresponded to the transverse diameter (Fig. 4). In 18 cases, in addition to this feature, a peculiar appearance was also noticed, as an oblique orientation both on latero-medial and antero-posterior planes, along the paraesophageal region. A cleavage plane between PTAs and thyroid gland was observed in 36 out of 46 adenomas (78.3 %). In 26 cases, an adipose cleavage plane was clearly evident; in ten cases of tight proximity of PTAs and thyroid gland, the India Ink artefact was detected (Fig. 5). A higher enhancement of PTAs in comparison with thyroid gland was observed in the first post-contrast sequence in 20 out of 46 cases (43.5 %) (Fig. 6). In all cases, the enhancement of adenomas in the first post-contrast sequences was also subjectively assessed as higher and faster than that of the lymph nodes of the same neck level. Results are summarised in Table 2.

T2-weighted IDEAL FSE imaging demonstrated both overall excellent fat suppression and image quality (average scores: 3.2 and 3.1, respectively). Post-contrast T1-weighted IDEAL images showed an intermediate grade of usefulness (average score 2.4) in 44/46 (95.7 %) cases. T1-weighted IDEAL sequence was extremely helpful in only one case, with low signal intensity on T2-weighted IDEAL FSE sequences. T2 IDEAL FSE out-of-phase sequences were evaluated as extremely helpful in only 16/46 adenomas (35 %); they were evaluated as marginally or very helpful in 21 cases and not helpful in nine PTAs. On a scale of 1 to 4, the mean value obtained in assessing the usefulness of this sequence was 2.8.

Surgical treatment and clinical follow-up

Eighteen of the 38 patients (47,4 %) underwent surgical intervention at our Institution (minimally invasive surgery in 12

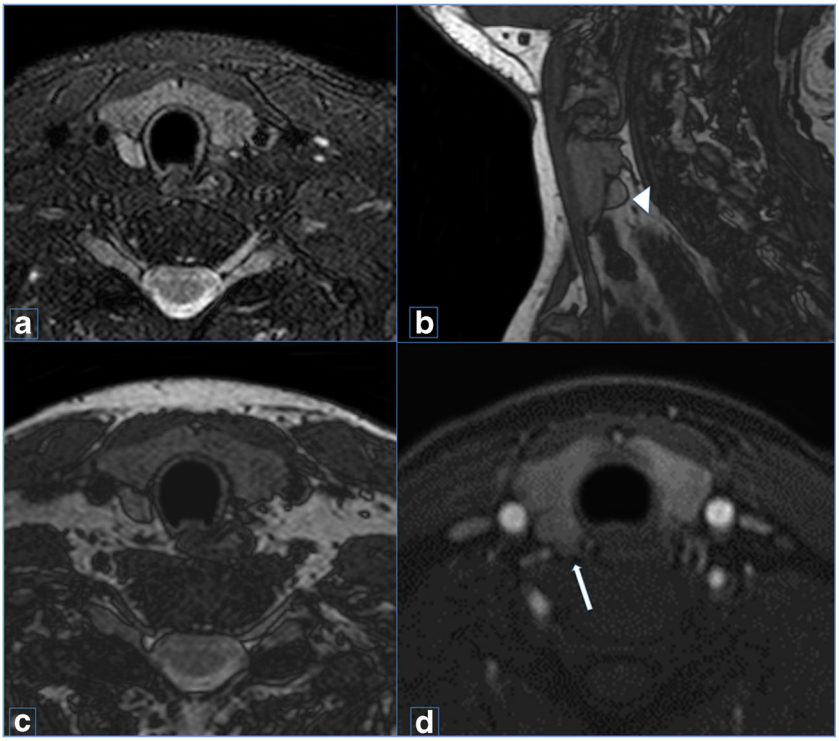

Fig. 2 A 45-year-old male. (*A*) Axial T2 IDEAL fat-suppressed and (*B, C*) sagittal and axial T2 out-phase images showing a homogeneously hyperintense PTA located in the right thyroid loggia, clearly separated from the thyroid gland, as confirmed by the *India-Ink artefact* (*arrowhead*). (*D*) Axial post-contrast T1WI showing mild enhancement of the PTA (*arrow*), similar to the enhancement of the thyroid gland

cases and open bilateral neck exploration in six cases), all in association with an intraoperative parathyroid hormone assay. The decision to operate was made within a multidisciplinary discussion.

In all 18 patients (24 PTAs), one or more enlarged parathyroid glands were found at surgery in the location identified by MRI and first level imaging techniques. At pathology, the diagnosis was PTA in all cases (24/24, 100 %). All the patients

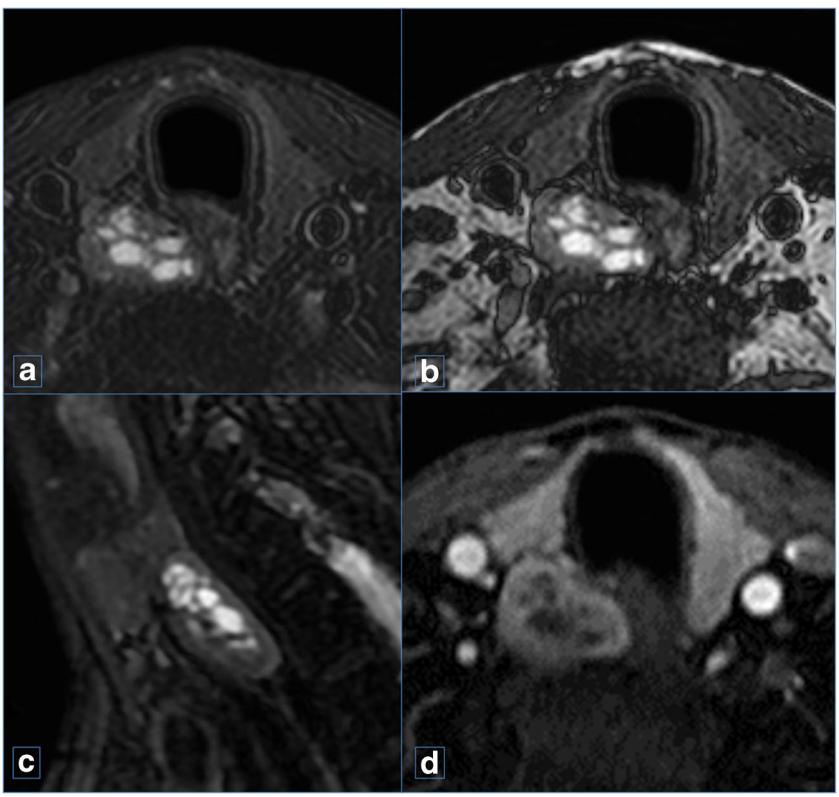

Fig. 3 A 54-year-old male. (*A*) Axial T2-weighted fat-suppressed, (*B*) axial T2 out-of-phase and (*C*) sagittal T2-weighted fat-suppressed images showing a right-sided "marbled" and elongated PTA, with internal cystic components, clearly separated from the thyroid gland. (*D*) Axial post-contrast T1WI showing a partial enhancement of the PTA, similar to that of the thyroid gland

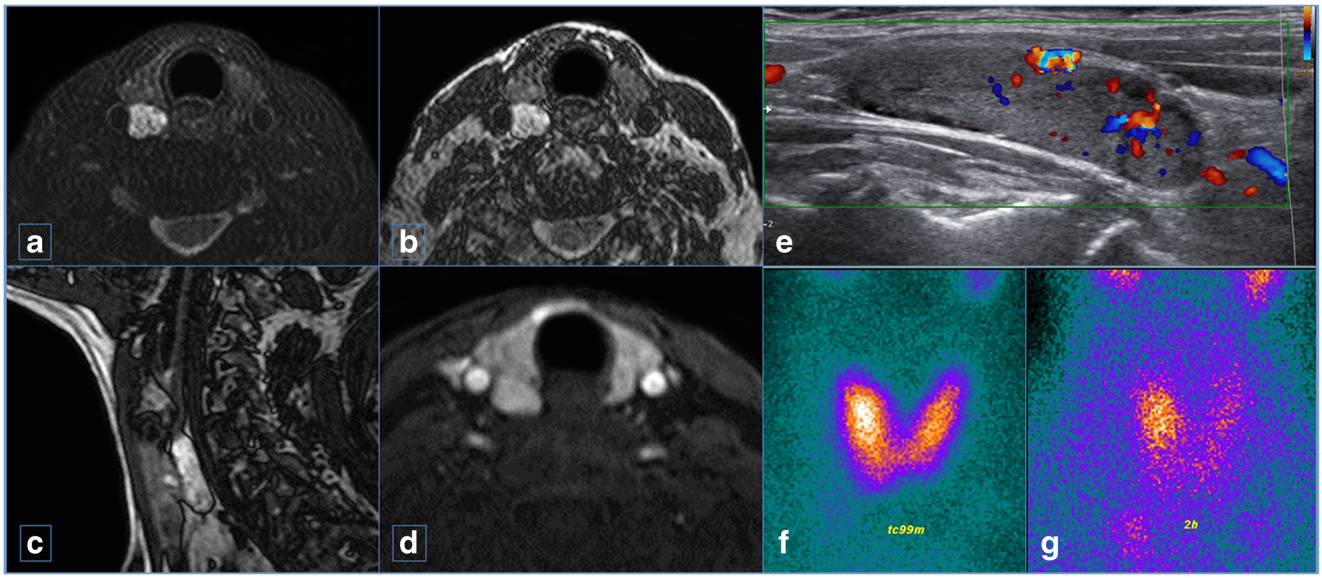

Fig. 4 A 74-year-old female. (*A*) Axial T2 IDEAL fat-suppressed and (*B*) axial and (*C*) sagittal T2-outphase images showing a heterogeneously hyperintense and elongated parathyroid adenoma, without any reliable cleavage plane with the thyroid gland. (*D*) Axial early post-contrast T1WI showing enhancement of the PTA, comparable to that of the thyroid gland. (*E*) US scan depicting the PTA as an oblong hypoechoic lesion with high Doppler signal. Sestamibi scan on (*F*) early and (*G*) delayed phases showing a large uptake area in the right parathyroid loggia

were seen 2 weeks postoperatively, and serum calcium, 25 hydroxy-vitamin D levels and parathyroid hormone levels were within the normal range; after this period, follow-up was limited to periodic evaluation of serum calcium levels [59].

In 20 patients, surgery was considered as not indicated. The main reasons for this decision were: asymptomatic hyperparathyroidism in old age (eight patients), serious comorbidities (seven patients), and patient refusal (five patients). Among these patients, 18 are currently being followed up at our institution and are undergoing medical therapy (administration of calcium and vitamin D appropriate for age and sex, and in some cases, bisphosphonates and calcimimetic drugs). The follow-up recommended for these patients is evaluation of serum calcium and creatinine levels every 6 months and bone mineral density every 3 months [59]. In addition, these patients are followed up with US every six-months; at present, all of them have undergone at least one follow-up US scan, confirming the size and location of the previously described PTAs (mean follow-up 12 months, range 6–18 months). Two patients were lost to follow-up.

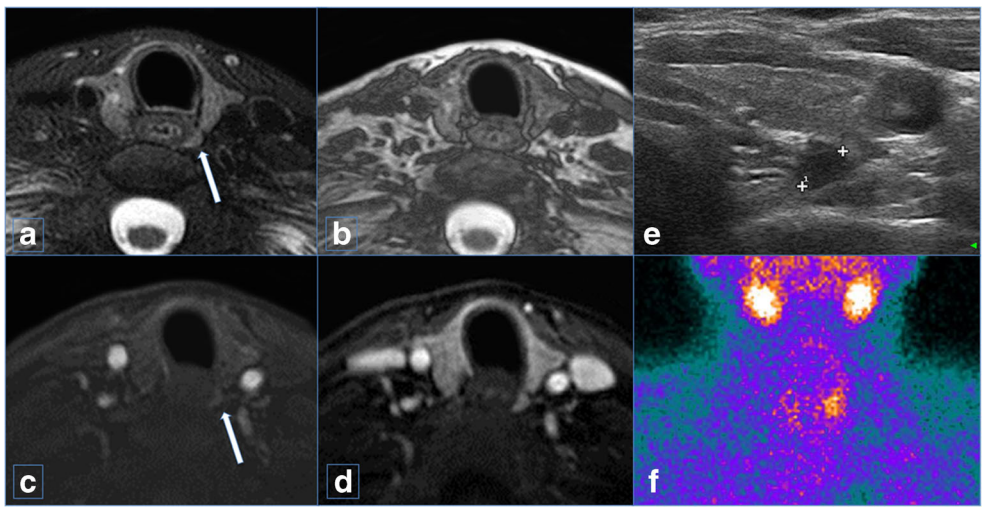

Fig. 5 A 61-year-old female. Axial (*A*) T2 IDEAL fat-suppressed and (*B*) T2-out-of-phase images showing a small left-sided, slightly hyperintense, paraoesophageal PTA (*arrow*), with associated *India-Ink artefact* suggesting a thin cleavage plane with the thyroid gland and the oesophagus. Axial (*C*) early (subtraction technique) and (*D*) delayed post-contrast T1WI showing, initially, mild and partial enhancement of the adenoma (*arrow*), and then complete enhancement, similar to that of the thyroid gland. (*E*) US and (*F*) sestamibi scans showing the PTA in the left thyroidal loggia, respectively, as an area of delayed uptake and as a paraoesophageal hypoechoic lesion

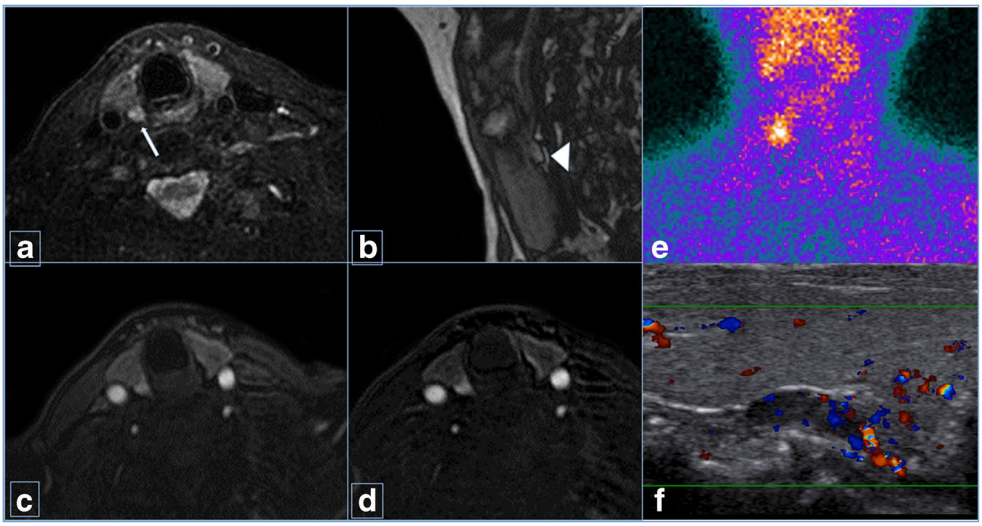

Fig. 6 A 77-year-old female. (*A*) Axial T2 IDEAL fat-suppressed and (*B*) sagittal T2-outphase images showing a hyperintense PTA, located posteriorly to the right lobe of the thyroid gland, separated from the thyroid gland by a thin cleavage plane (*arrowhead*). (*C*) Axial post-contrast T1WI and (*D*) subtraction images showing an *early and avid enhancement*, clearly higher than that of thyroid. (*E*) Sestamibi scan and (*F*) US colour-Doppler demonstrating the PTA in the right thyroid loggia, respectively, as an area of delayed uptake and as a hypoechoic lesion with high Doppler signal

Discussion

Accurate preoperative localisation of PTAs permits the use of minimally invasive approaches in parathyroid surgery, which, compared to bilateral neck exploration and repeated surgery, are more efficient and less expensive [12–17]. If US and sestamibi scan fail to localise PTA [18, 22, 23], a second line imaging technique, such as CT and MRI, is usually suggested in order to avoid bilateral neck exploration [60, 61].

Recently, the use of 4D CT in the detection of PTA was evaluated, with discordant results [62–65]. MRI has been more rarely used in comparison with CT; MRI signal features of PTAs, such as low T1 signal, high T2 signal and contrast enhancement, previously described at 1.5 T, were not invariably observed and were not peculiar to PTAs [66, 67]. In fact, other entities located in the same anatomical sites, such as lymph nodes and exophytic thyroid nodules, may show high T2 signal [68]. The aim of our study was not to evaluate the diagnostic accuracy of MRI in detecting PTAs, but to identify common MRI features of PTAs, in order to facilitate their depiction and to improve the diagnostic performance of the technique in the near future.

From a pathological point of view, PTA is characterised by a lack of adipose tissue; therefore, the intrinsic hyperintensity seen on T2-weighted sequences, especially visible after fat-suppression, most likely depends on the presence of non-fat components [69, 70]. To better evaluate the entire neck region and to identify structures with high T2 signal, it is necessary to obtain a homogeneous fat suppression, which is notoriously challenging in the neck region. Recently, advances in chemical shift-based water–fat separation methods, commercially known as IDEAL, have been developed and implemented on 3.0 T MRI units [50–52]. These sequences provide excellent fat suppression with signal-to-noise ratio superior to that of short-tau inversion recovery sequences (STIR). Using IDEAL sequences, Grayev et al. [54] recently reported a low sensitivity (64 %), but had the ability to detect a few adenomas that were missed by sestamibi. We reported high frequency (95.7 %) of hyperintensity on T2-weighted IDEAL FSE images, suggesting that a high T2 signal is the feature to be used to localise a structure that is suspected of representing a PTA.

In our study, 65.2 % of PTAs showed a patchy hyperintensity (i.e., a "marbled" appearance); many of these adenomas were larger than 15 mm in the maximum diameter. It is reported in the literature that large adenomas often display haemorrhagic foci, cholesterol clefts and fibrosis that may be the cause of the marbled appearance on T2 sequences [71]. This characteristic allows for differentiation of large adenomas from lymph nodes, but not from exophytic thyroid nodules. Also, the elongated morphology observed in 82.6 % of PTAs in our study is

Table 2 Frequent 3 T MRI features of parathyroid adenomas

	Hyperintensity	Marbled appearance	Elongated morphology	Cleavage Plane	Early enhancement
PTA (*n*=46)	44	30	38	36	20
%	95.7	65.2	82.6	78.3	43.5

common in lymph nodes, and therefore cannot be considered as specific of adenoma. Despite this, it was noticed that 18 adenomas showed a peculiar appearance, which may be described as an oblique orientation both on latero-medial and antero-posterior planes, extending along the paraoesophageal region.

An additional advantage of the water–fat separation technique used in our study is that in-phase and out-of-phase images, and fat-only and water-only images, are obtained through a single acquisition. Out-of-phase images are characterised by a chemical shift type 2 artefact, the so-called "India ink artefact", which represents the black boundary artefact generated by a signal drop in voxels containing both fat and non-fat components. In the case of tight proximity of PTA and thyroid gland, this artefact can enable a clear depiction of a thin adipose cleavage plane, thus supporting the differential diagnosis between PTAs and exophytic thyroid nodules; this feature is not useful in differentiating PTAs and lymph nodes [58, 72]. In our study, in 78.3 % of cases, a cleavage plane between adenoma and thyroid was detected, thus confirming that the "India ink artefact" is an important feature in identifying a structure as separate from the thyroid gland; these data influenced the radiologists' assessment of usefulness of the T2 IDEAL FSE out-of-phase sequences, which was graded as 2.8 on a scale of 1 to 4 (1=not helpful, 2=marginally helpful, 3=very helpful, 4=extremely helpful).

Strong and rapid enhancement is a well-known characteristic of PTAs, advocated for better detection of PTAs by several authors [42–45]. In our series, however, only 43.5 % of PTAs demonstrated faster and higher enhancement compared to normal thyroid. To our knowledge, an agreement about a post-contrast sequence protocol has not been reached. The previously proposed use of TRICKS led to an increased temporal resolution, but with decreased spatial resolution [51], and to just a modest improvement in PTA detection in comparison with T2-weighted IDEAL FSE sequences [54]. Our post-contrast protocol was optimised in order to perform quite rapid sequences, at the same time maintaining a high spatial resolution. Even with this optimisation, post-contrast sequences did not significantly improve the detection of PTAs. We noticed that in the majority of cases (44/46; 95.6 %), adenomas were already satisfactorily depicted on pre-contrast sequences; this observation was in line with the high rate of T2-hyperintense PTAs and low usefulness shown by the post-contrast T1-weighted images. If this observation is confirmed in larger studies, contrast media administration may be used only in cases where there is a residual diagnostic doubt after non-enhanced sequences.

This study has some limitations. Firstly, surgical confirmation was not available for all patients included in the study. Our confidence in the diagnosis of PTA was based on clinical findings, lab tests, both positive and concordant US and sestamibi scans, and correlation between MRI and these two imaging techniques. With regard to this choice, radiologists and clinicians involved in the management of PHPT patients are aware that the low rate of surgical confirmation is a well-known issue in this group of patients. Most patients are treated with medical therapy only or undergo surgery after a long period of time and in other hospitals (in such cases, pathology results may be not available or are inaccurately reported). The old age group of patients may also play a role in the decision to avoid surgery.

We believe that we should not exclude all non-surgical patients from a study on MRI of PTAs, because this would generate a strong selection bias. In addition, since positive US and sestamibi scans are currently considered in clinical practice as a sufficient prerequisite to submit patients to surgery, we believe that this is a good reason to consider these two imaging techniques as a reasonable gold standard in a purely descriptive study. Furthermore, the aim of the study was to describe the common MRI features of typical adenomas, and how to perform an optimal MR examination, and not to evaluate the diagnostic accuracy of MRI in detecting PTAs. For the same reason, readers were aware of previous imaging results (to be sure that they were looking at PTAs and not at lymph nodes or thyroid nodules).

Another potential limitation pertains to our selection criteria; these criteria, requiring positive US and sestamibi scans, may have potentially created bias for example, leading to the inclusion of patients with large adenomas; however, the average size of the PTAs observed in our study was less that 15 mm (14.5x8.5x9.5 mm). An additional limitation regards the semi-quantitative method used for the assessment of T2-signal intensity and contrast enhancement (subjective evaluation, performing ROIs in case of doubt). In the next protocol, we will use quantitative methods and post-contrast time-to-intensity curves in order to better evaluate these features (these methods might be useful even in patients without normal thyroid parenchyma available for comparison, such as in patients with multinodular goiter).

Another limitation of this study was that all the PTAs were located in eutopic sites, hence, MRI features observed in typical adenomas need to be confirmed in ectopic adenomas, especially in the mediastinal ones. In order to accurately evaluate the same features in these ectopic PTAs, we are planning to add to our standard protocol a triggered sequence dedicated to the visualisation of the mediastinum.

Conclusion

The most common features of PTAs recognised in our study allowed for a differential diagnosis with other normal structures or pathological tissues of the neck. We agree with previous authors [54] and suggest the use of MRI as a second-line method in the preoperative detection of PTAs, in the case of negative or discordant first-line imaging modalities. It is

necessary to integrate the use of new sequences performed on a 3.0-T MR scanner with increased radiological skills, in order to achieve high accuracy in presurgical localisation of PTAs by MRI.

Acknowledgments The scientific guarantor of this publication is prof. Carlo Catalano. The authors of this manuscript declare no relationships with any companies, whose products or services may be related to the subject matter of the article. The authors state that this work has not received any funding. No complex statistical methods were necessary for this paper. Institutional Review Board approval was obtained. Written informed consent was obtained from all subjects (patients) in this study. Methodology: prospective, observational study, performed at one institution.

References

1. Fraser WD (2009) Hyperparathyroidism. Lancet 374:145–158
2. Bilezikian JP, Silverberg SJ (2004) Clinical practice. Asymptomatic primary hyperparathyroidism. N Engl J Med 350:1746–1751
3. Ruda JM, Hollenbeak CS, Stack BC Jr (2005) A systematic review of the diagnosis and treatment of primary hyperparathyroidism from 1995 to 2003. Otolaryngol Head Neck Surg 132:359–372
4. Akerstrom G, Malmaeus J, Bergstrom R (1984) Surgical anatomy of human parathyroid glands. Surgery 95:14–21
5. Eigelberger MS, Cheah WK, Ituarte PH et al (2004) The NIH criteria for parathyroidectomy in asymptomatic primary hyperparathyroidism: are they too limited? Ann Surg 239:528–535
6. Silverberg SJ, Clarke BL, Peacock M et al (2014) Current issues in the presentation of asymptomatic primary hyperparathyroidism: proceedings of the fourth international workshop. J Clin Endocrinol Metab 99:3580–3594
7. Bilezikian JP, Brandi ML, Eastell R et al (2014) Guidelines for the management of asymptomatic primary hyperparathyroidism: summary statement from the fourth international workshop. J Clin Endocrinol Metab 99:3561–3569
8. Wang CA (1976) The anatomic basis of parathyroid surgery. Ann Surg 183:271–275
9. Okuda I, NakajimaY MD et al (2010) Diagnostic localization of ectopic parathyroid lesions: developmental consideration. Jpn J Radiol 28:707–713
10. Low RA, Katz AD (1998) Parathyroidectomy via bilateral cervical exploration: a retrospective review of 866 cases. Head Neck 20: 583–587
11. Udelsman R (2002) Six hundred fifty-six consecutive explorations for primary hyperparathyroidism. Ann Surg 235:665–670
12. Miccoli P, Bendinelli C, Berti P et al (1999) Video-assisted versus conventional parathyroidectomy in primary hyperparathyroidism: a prospective randomized study. Surgery 126:1117–1122
13. Howe JR (2000) Minimally invasive parathyroid surgery. Surg Clin N Am 80:1399–1426
14. Miccoli P, Barellini L, Monchik JM et al (2005) Randomized clinical trial comparing regional and general anaesthesia in minimally invasive video-assisted parathyroidectomy. Br J Surg 92:814–818
15. Grant CS, Thompson G, Farley D et al (2005) Primary hyperparathyroidism surgical management since the introduction of minimally invasive parathyroidectomy: Mayo Clinic experience. Arch Surg 140:472–478
16. Barczynski M, Cichon S, Konturek A et al (2006) Minimally invasive video-assisted parathyroidectomy versus open minimally invasive parathyroidectomy for a solitary parathyroid adenoma: a prospective, randomized, blinded trial. World J Surg 30:721–731
17. Chen H, Mack E, Starling JR (2005) A comprehensive evaluation of perioperative adjuncts during minimally invasive parathyroidectomy: which is most reliable? Ann Surg 242:375–383
18. Tublin ME, Pryma DA, Yim JH et al (2009) Localization of parathyroid adenomas by sonography and technetium Tc 99m sestamibi single-photon emission computed tomography before minimally invasive parathyroidectomy: are both studies really needed? J Ultrasound Med 28:183–190
19. Vignali E, Picone A, Materazzi G et al (2002) A quick intraoperative parathyroid hormone assay in the surgical management of patients with primary hyperparathyroidism: a study of 206 consecutive cases. Eur J Endocrinol 146:783–788
20. Boudou P, Ibrahim F, Cormier C et al (2005) Third- or second-generation parathyroid hormone assays: a remaining debate in the diagnosis of primary hyperparathyroidism. J Clin Endocrinol Metab 90:6370–6372
21. Carneiro-Pla D (2009) Effectiveness of "office"-based, ultrasound-guided differential jugular venous sampling (DJVS) of parathormone in patients with primary hyperparathyroidism. Surgery 146: 1014–1020
22. Johnson NA, Tublin ME, Ogilvie JB (2007) Parathyroid imaging: technique and role in the preoperative evaluation of primary hyperparathyroidism. AJR 188:1706–1715
23. Phillips CD, Shatzkes DR (2012) Imaging of the parathyroid glands. Semin Ultrasound CT MR 33:123–129
24. Mohebati A, Shaha AR (2012) Imaging techniques in parathyroid surgery for primary hyperparathyroidism. Am J Otolaryngol 33: 457–468
25. Cakala E, Cakir E, Dillib A et al (2012) Parathyroid adenoma screening efficacies of different imaging tools and factors affecting the success rates. Clin Imaging 36:688–694
26. Reeder SB, Desser TS, Weigel RJ et al (2002) Sonography in primary hyperparathyroidism: review with emphasis on scanning technique. J Ultrasound Med 21:539–552
27. Gilat H, Cohen M, Feinmesser R et al (2005) Minimally invasive procedure for resection of a parathyroid adenoma: the role of preoperative high resolution ultrasonography. J Clin Ultrasound 33: 283–287
28. Vitetta GM, Neri P, Chiecchio A et al (2014) Role of ultrasonography in the management of patients with primary hyperparathyroidism: retrospective comparison with technetium-99m sestamibi scintigraphy. J Ultrasound 31:1–12
29. Van Husen R, Kim LT (2004) Accuracy of surgeon-performed ultrasound in parathyroid localization. World J Surg 28:1122–1126
30. Sofferman RA, Nathan MH, Fairbank JT et al (1996) Preoperative technetium Tc 99m sestamibi imaging: paving the way to minimal-access parathyroid surgery. Arch Otolaryngol Head Neck Surg 122: 369–374
31. Allendorf J, Kim L, Chabot J et al (2003) The impact of sestamibi scanning on the outcome of parathyroid surgery. J Clin Endocrinol Metab 88:3015–3018
32. Palestro JC, Tomas MB, Tronco GG (2005) Radionuclide imaging of the parathyroid glands. Semin Nucl Med 35:266–276
33. Nichols KJ, Tomas MB, Tronco GG et al (2008) Preoperative parathyroid scintigraphic lesion localization: accuracy of various types of readings. Radiology 248:221–232
34. Lumachi F, Zucchetta P, Marzola MC et al (2000) Advantages of combined technetium-99m-sestamibi scintigraphy and high-resolution ultrasonography in parathyroid localization: comparative study in 91 patients with primary hyperparathyroidism. Eur J Endocrinol 143:755–760
35. Patel CN, Salahudeen HM, Lansdown M et al (2010) Clinical utility of ultrasound and 99mTc sestamibi SPECT/CT for preoperative localization of parathyroid adenoma in patients with primary hyperparathyroidism. Clin Radiol 65:278–287

36. Kettle AG, O'Doherty MJ (2006) Parathyroid imaging: how good is it and how should it be done. Semin Nucl Med 36:206–211
37. Krudy AG, Doppman JL, Brennan MF et al (1981) The detection of mediastinal parathyroid glands by computed tomography, selective arteriography, and venous sampling: an analysis of 17 cases. Radiology 140:739–744
38. van Dalen A, Smit CP, van Vroonhoven TJMV et al (2001) Minimally invasive surgery for solitary parathyroid adenomas in patients with primary hyperparathyroidism: role of US with supplemental CT. Radiology 220:631–639
39. Lumachi F, Tregnaghi A, Zucchetta P et al (2004) Technetium-99m sestamibi scintigraphy and helical CT together in patients with primary hyperparathyroidism: a prospective clinical study. Br J Radiol 77:100–103
40. Rodgers SE, Hunter GJ, Hamberg LM et al (2006) Improved preoperative planning for directed parathyroidectomy with 4-dimensional computed tomography. Surgery 140:932–940
41. Mortenson MM, Evans DB, Lee JE et al (2008) Parathyroid exploration in the reoperative neck: improved preoperative localization with 4D-computed tomography. J Am Coll Surg 206:888–895
42. Gotway MB, Higgins CB (2000) MR imaging of the thyroid and parathyroid glands. Magn Reson Imaging Clin N Am 8:163–182
43. Lopez Hanninen E, Vogl TJ, Steinmuller T et al (2000) Preoperative contrast-enhanced MRI of the parathyroid glands in hyperparathyroidism. Investig Radiol 35:426–430
44. Gotway MB, Reddy GP, Webb WR et al (2001) Comparison between MR imaging and 99mTc MIBI scintigraphy in the evaluation of recurrent or persistent hyperparathyroidism. Radiology 18:783–790
45. Kabala JE (2008) Computed tomography and magnetic resonance imaging in diseases of the thyroid and parathyroid. Eur J Radiol 66: 480–492
46. Michel L, Dupont M, Rosière A et al (2013) The rationale for performing MR imaging before surgery for primary hyperparathyroidism. Acta Chir Belg 113:112–122
47. Stanisz GJ, Odrobina EE, Pun J et al (2005) T1, T2 relaxation and magnetization transfer in tissue at 3T. Magn Reson Med 54:507–512
48. Barth MM, Smith MP, Pedrosa I et al (2007) Body MR imaging at 3.0 T: understanding the opportunities and challenges. Radiographics 27:1445–1463
49. Reeder SB, Pineda AR, Wen Z et al (2005) Iterative decomposition of water and fat with echo asymmetry and least-squares estimation (IDEAL): application with fast spin-echo imaging. Magn Reson Med 54:636–644
50. Ma J, Singh SK, Kumar AJ et al (2004) T2-weighted spine imaging with a fast three-point Dixon technique: comparison with chemical shift selective fat suppression. J Magn Reson Imaging 20:1025–1029
51. Barger AV, DeLone DR, Bernstein MA et al (2006) Fat signal suppression in head and neck imaging using fast spin-echo IDEA L technique. AJNR Am J Neuroradiol 27:1292–1294
52. Reeder SB, McKenzie CA, Pineda AR et al (2007) Water–fat separation with IDEAL gradient-echo imaging. J Magn Reson Imaging 25:644–652
53. Korosec FR, Frayne R, Grist TM et al (1996) Time-resolved contrast-enhanced 3D MR angiography. Magn Reson Med 36:345–351
54. Grayev AM, Perlman SB, Gentry LR (2012) Presurgical localization of parathyroid adenomas with magnetic resonance imaging at 3.0 T: an adjunct method to supplement traditional imaging. Ann Surg Oncol 19:981–989
55. Auffermann W, Guis M, Tavares NJ et al (1989) MR signal intensity of parathyroid adenomas: correlation with histopathology. AJR Am J Roentgenol 153:873–876
56. Wieneke JA, Smith A (2008) Parathyroid adenoma. Head Neck Pathol 2:305–308
57. Busse RF, Brau AC, Vu A, Michelich CR et al (2008) Effects of refocusing flip angle modulation and view ordering in 3D fast spin echo. Magn Reson Med 60:640–649
58. Israel GM, Hindman N, Hecht E et al (2005) The use of opposed-phase chemical shift MRI in the diagnosis of renal angiomyolipomas. AJR Am J Roentgenol 184:1868–1872
59. The American Association of Clinical Endocrinologists and the American Association of Endocrine Surgeons position statement on the diagnosis and management of primary hyperparathyroidism. (2005) Endocr Pract 11(1):49–54
60. Lubitz CC, Stephen AE, Hodin RA et al (2012) Preoperative localization strategies for primary hyperparathyroidism: an economic analysis. Ann Surg Oncol 13:4202–4209
61. Cheung K, Wang TS, Farrokhyar F et al (2012) A meta-analysis of preoperative localization techniques for patients with primary hyperparathyroidism. Ann Surg Oncol 19:577–583
62. Kutler DI, Moquete R, Kazam E et al (2011) Parathyroid localization with modified 4D-computed tomography and ultrasonography for patients with primary hyperparathyroidism. Laryngoscope 121: 1219–1224
63. Chazen JL, Gupta A, Dunning A et al (2012) Diagnostic accuracy of 4D-CT for parathyroid adenomas and hyperplasia. AJNR 33: 429–433
64. Hoang JK, Sung WK, Bahl M (2014) How to Perform Parathyroid 4D CT: tips and traps for technique and interpretation. Radiology 270:15–24
65. Mahajan A, Starker LF, Ghita M et al (2012) Parathyroid four-dimensional computed tomography: evaluation of radiation dose exposure during preoperative localization of parathyroid tumors in primary hyperparathyroidism. World J Surg 36:1335–1339
66. Numerow LW, Morita ET, Clark OH et al (1995) Hyperparathyroidism: a comparison of sestamibi scintigraphy, MRI, and ultrasonography. J Magn Reson Imaging 5:702–708
67. McDermott VG, Fernandez RJ, Meakem TJ 3rd et al (1996) Preoperative MR imaging in hyperparathyroidism: results and factors affecting parathyroid detection. AJR 166:705–710
68. Ernst O (2009) Hyperparathyroidism: CT and MR findings. J Radiol 90:409–412
69. Ghandur-Mnaymneh L, Kimura N (1984) The parathyroid adenoma: a histopathologic definition with a study of 172 cases of primary hyperparathyirodism. Am J Pathol 115:70–83
70. Genc H, Morita E, Perrier ND et al (2003) Differing histologic findings after bilateral and focused parathyroidectomy. J Am Coll Surg 196:535–540
71. Carlson D (2010) Parathyroid pathology hyperparathyroidism and parathyroid tumors. Arch Pathol Lab Med 134:1639–1644
72. Turner HE, Harris AL, Melmed S et al (2013) Angiogenesis in endocrine tumors. Endocr Rev 24:600–632